Biomedical Research 2020; 31 (2): *ISSN 0970-938X*
www.biomedres.info

Loss of *Dnm1* gene in mitochondria results in changes of microtubuland chromosomes dynamics in *Schizosaccharomyces pombe.*

Xiumei Tan[1], Rongmei Yuan[1], Xiang Ding[2], Yilling Haou [1*]

[1]Key Laboratory of Southwest China Wildlife Resources Conservation (Ministry of Education), College of Life Sciences, China West Normal University, Shida Road, Nanchong, Sichuan Province 637009, China

[2]College of environmental science and Engineering, China West Normal University, Shida Road, Nanchong, Sichuan Province 637009, China

Abstract

Mitochondria are dynamic organelles that undergo fission and fusion cycles. The major mitochondrial fission protein is dynamin-related Drp1 GTPase (*Dnm1* in yeast). Here, the model of *Schizosaccharomyces pombe* was used to explore the effect of *Dnm1* gene deletion on cell dynamics in mitosis. The *Dnm1* gene deletion can cause slow growth, and sporogenesis abnormality of Schizosaccharomyces pombe, and the microtubules number and length abnormality at interphase. The *Dnm1* gene deletion can also affect the growth rate and time of spindle in the metaphase and anaphase, and affect the fluorescence intensity of spindle in the prophase and metaphase. At the same time, spindle microtubule organization and dynamics were different in *Dnm1*△ cells compared with wild type cells. Spindle length statistics showed that there was delayed spindle breakage in *Dnm1*△ cells. Live-cell imaging was performed on mutant strains to observe two distinct chromosome behaviors: normal and lagging. Analysis of coenzyme, intermediates and energy in energy metabolism indicated that some abnormalities occurred after the deletion of the *Dnm1* gene. It is concluded that the loss of *Dnm1* gene from mitochondria resulted in mitochondrial dynamics deficiency which will contribute to the spindle maintenance deficiency, chromosome segregation deficiency, spindle breakage deficiency, coenzyme deficiency, intermediate metabolite deficiency and ATP production deficiency.

Keywords: Mitochondria, *Dnm1* gene, Cell cycle, Dynamics, Mitosis.

Accepted on April 24, 2020

Introduction

Mitochondria are a kind of dynamic organelle and undergo a cycle of division and fusion [1-5]. Therefore, the regulatory balance between division and fusion seems to be crucial for the control of mitochondrial morphogenesis [6]. In fact, mitochondrial division and fusion kinetics, as well as proteins that control these processes (from yeast to humans), are essential, and their disorders are associated with serious human diseases, including Charcot-Marie-Tooth disease type 6, Beckwith-Wiedemann syndrome, neurodegenerative diseases, Charcot-Marie-Tooth disease axonal type 2S, multiple symmetric lipomatosis and microcephaly [7-15].

The dynamin-related protein of mitochondria is mainly Drp1 GTPase (*Dnm1* in yeast) [16-18]. GTPase of dynamin family is similar in structure, with GTP binding, middle and GTPase effect domains, but different in function. It has been reported that the mitochondria in *Dnm1*Δ present as highly interconnected tubules forming a network structure or thick bundle like tubules, which indicates that *Dnm1* is necessary for mitochondrial fission [19]. *Dnm1* mediates mitochondrial fission at interphase growth and at cell division during mitosis [20]. In budding yeast Saccharomyces cerevisiae, *Dnm1*p (known as DLP1, Drp1, or dvlp1 in other species), together with net2p / gag3p / mdv1p / fis2p, is captured by fis1p / mdv2p and mediates mitochondrial division [21]. In addition, the repetitive role of *Dnm1* with vps1 in peroxisome biogenesis under cell cycle regulation was also reported [22].

Cell replication involves a series of highly regulated and evolutionarily conserved complex events, called "cell cycle"[23]. Abnormalities in cell cycle have a serious impact and can lead to cancer growth. A detailed understanding of cell cycle and its regulation can identify other targets for cancer treatment. *Schizosaccharomyces pombe* (fission yeast) is a unicellular organism, which is easy to be genetically manipulated and has many cell cycle characteristics similar to those of metazoan cells [24]. It is an important model organism for studying cell cycle and checkpoint control [25]. In this paper, the effect of *Dnm1* gene deletion on cell mitotic dynamics was studied by using the model of *Schizosaccharomyces pombe* (fission yeast).

Materials and Methods

S. pombe strains construction

Yeast genetics was carried out as previously described [26], and yeast strains were created by random spore digestion. Yeast culture media were purchasetd from For Medium (Norfolk, UK). All strains used in this study are listed in Table 1.

Table 1. *List of strains.*

Strain	Genotype	Figure
PT.286	Wt: ade6.210 leu1.32 ura4.D18 h-	1-7
PT.287	Wt: ade6.210 leu1.32 ura4.D18 h+	1-7
PT.917	Wt: mC-Atb2: leu1.32 h-	\
PT.2167	Wt: Hht2-GFP: leu1.32 ura4.D18 h+	\
HY 4	Wt: Hht2-GFP: ura4.D18 mC-Atb2: leu1.32 KanR h-	1-7
HY 5	Wt: Hht2-GFP: ura4.D18 mC-Atb2: leu1.32 KanR h+	1-7
HY 1933-1	Dnm1Δ: KanR h-	1-7
HY 1933-2	Dnm1Δ: KanR h+	1-7
HY 1933-4	Dnm1Δ: Hht2-GFP: ura4.D18 mC-Atb2: leu1.32 KanR h-	1-7
HY 1933-4	Dnm1Δ: Hht2-GFP: ura4.D18 mC-Atb2: leu1.32 KanR h+	1-7

Microscopy

Live cell imaging was carried out at room temperature 25°C. A spinning-disc confocal microscope equipped with a Nikon PlanApo 100×/1.40 NA objective and the Photometrics CoolSNAP HQ2 CCD camera was used [27]. MetaMorph 7.5 (http://www.moleculardevices.com) was used to acquire and process all images. For high temporal resolution, images were acquired at 300 – 500 ms exposure for GFP/mCherry, 60-sec intervals, 90 min total time for 11 optical sections of 0.5 μm spacing.

Analysis method of energy metabolites

The cells were cultured in YE5S medium, 25°C for 3 days. The cells were washed three times with cold PBS and collected in a 1.5 ml centrifuge tube, frozen in liquid nitrogen, stored at -80°C, after centrifuged with 3000 g at 4°C for 5 minutes. The collected cells were sent to Shanghai applied protein Technology Co. Ltd. to be analyzed for metabonomics by LC-MS.

Data analysis

All data were expressed as mean ± SD, and the significant difference between the experimental group and the control group was statistically analyzed by one-way ANOVA using SPSS 17 software. * $p<0.05$, represents a significant difference, and ** $P<0.01$ represents a extremely significant difference, respectively. All plots were created using Kaleidagraph 4.0 (http://www.synergy.com). Box plots show all individual data, and the plots enclose 50% of the data in the box with the median value displayed as a line. The lines extending from the top and bottom of each box mark the minimum and maximum values within the data set that fall within an acceptable range. Outliers are displayed as individual points.

Results

The effect of Dnm1 gene deletion on the cell growth, morphology and number of microtubule and ascospores

The cell growth results indicated that there is little difference of the growth rate between wild type and *Dnm1*Δ cells at 25°C for 0-6 hour. After 6 hours, the growth rate of wild type increased, while that of *Dnm1*Δ cells has been extremely slow. After 12 hours, the OD 595 of wild type has reached 0.625, but the OD 595 of *Dnm1*Δ cells was only 0.202, which is quite different from the wild type cells (Figure 1a). The results showed that *Dnm1* gene deletion can cause slow growth of *Schizosaccharomyces pombe*. Number of ascospores produced by wild type and *Dnm1*Δ cells as shown in (Figures 1b and 1c). The results showed that 99.20 ± 0.00%, 0.53 ± 0.31% and 0.27 ± 0.31% of wild-type cells produce four, three and two ascospores (n=500), respectively, while 95.07 ± 0.81%, 4.73 ± 0.64% and 0.00 ± 0.00% of *Dnm1*Δ cells produce four, three and two ascospores, respectively, in which there had extremely significant difference ($P<0.01$) in the number of four and three ascospores (Figures 1b and 1c). There was no difference in ascospore morphology between wild type and *Dnm1*Δ cells, which showed that *Dnm1* gene and its encoded protein could affect the production number of ascospores of *Schizosaccharomyces pombe*, but could not affect the spore morphology.

Number of microtubules in wild type and *Dnm1*Δ cells in mitotic interphase as shown in Figures 1d and 1e. The results showed that 31.67 ± 2.89%, 55.00 ± 5.00%, and 13.33 ± 5.77% of wild-type cells have three, four and five microtubules, respectively, while 13.33 ± 2.88%, 63.34 ± 5.77% and 23.33 ± 7.63% of *Dnm1*Δ cells have three, four, five microtubules, respectively, in which there had extremely significant difference ($P<0.01$) in the number of three microtubules between wild type and *Dnm1*Δ cells. Statistical results of microtubule length in mitotic interphase cells showed that microtubule length of wild type and *Dnm1*Δ cells were 5.13 ± 1.44 μm and 5.97 ± 2.14 μm, respectively, which had extremely significant difference in the two groups (Figure 1f). The results showed that loss of *Dnm1* gene will cause the length of microtubules in cells tends to increase.

The microtubule dynamics of wild type cells and *Dnm1*Δ cells during mitotic interphase was analyzed. The results showed that the MT (Microtubule) of wild-type cells grew at 1.50 ± 0.56 μm/min (n=10) and shrunk at 1.40 ± 0.30 μm/min (n=10), and the MT dwell time was 1.21 ± 0.21 min (n=10). In contrast, the MT of *Dnm1*Δ cells grew at 1.57 ± 0.85 μm/min

(n=10) and shrunk at 1.21 ± 0.47 μm/min (n=10), and the MT dwell time was 1.16 ± 0.31 min (n=10) (Figures 1g-1j). The results indicated that there were no different of microtubule dynamics during mitotic interphase between wild type and *Dnm1*Δ cells.

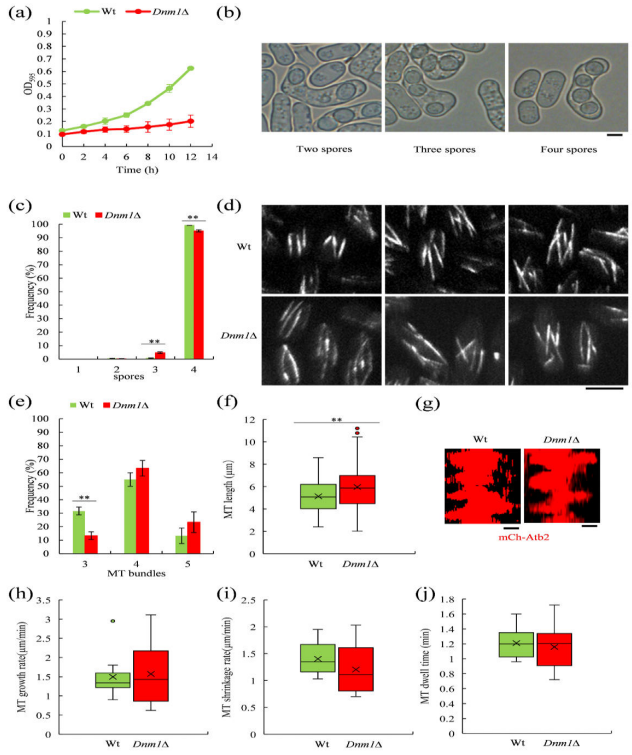

Figure 1. *The effect of Dnm1 gene deletion on the cell growth, morphology and number of microtubule and ascospores a The growth curves of wild type and Dnm1Δ cells cultured at 25°C. Notes: Data represented as mean ± SD (n=3, the experiment was repeated three times). b Morphology results of ascospores in Dnm1Δ cells. Scale bar: 5 μm. c Statistical analysis of spore number of wild type and Dnm1Δ cells (n=500, n is the number of cells). Notes: Data represented as mean ± SD. ** P<0.01. d Microtubule morphology of wild type and Dnm1Δ cells in mitotic interphase. Scale bar: 5 μm. e Statistical analysis of the number of microtubules of wild type and Dnm1Δ cells in the mitotic interphase (n=20; n is the number of cells). Choose the time of 8 minutes in mitotic interphase as the observation time of microtubule morphology. Take the maximum number of microtubules in each cell as the final microtubules number, and the maximum microtubule length of each microtubule as the final microtubule length. Use the same VANILE ratio in FIJI to reduce the statistical error of fluorescent dye. Notes: Data represented as mean ± SD. ** P<0.01. f Statistical analysis of the length of wild type and Dnm1Δ cells in the mitotic interphase (n=80; n is the number of microtubules). ** P<0.01. g Microtubule dynamics of wild type cells and Dnm1Δ cells during mitotic interphase. Scale bar: 2 μm. h Statistical analysis of MT growth rate in wild type and Dnm1Δ cells (n=10, n is microtubule number). i Statistical analysis of MT shrinkage rate in wild type and Dnm1Δ cells (n=10, n is microtubule number). j Statistical analysis of MT dwell time in wild type and Dnm1Δ cells (n=10, n is microtubule number)*

The effect of Dnm1 gene deletion on spindle and cell length during cell mitosis

During mitosis, the SPBs (Spindlepolebody) organize the mitotic spindle for chromosomal segregation. The mitotic spindle has three distinct phases of elongation, corresponding to distinct stages of mitosis. The SPBs also organize the astral MTs, which function similarly to interphase MTs in nuclear and spindle positioning. The mC-Atb2 (α-tubulin) and Hht2-

GFP (Nucleosomal histone) were used as a detection signal for prophase and metaphase to monitor spindle elongation and chromosome segregation dynamics in cell mitosis of wild-type cells and *Dnm1*Δ cells. Wild-type cells exhibited stereotypical three-phase spindle elongation kinetics, corresponding to prophase (phase I), metaphase (phase II), and anaphase A (chromatid separation) and B (spindle elongation) (Figure 2a). There are some abnormal situations in *Dnm1*Δ cells. Spindle length statistics showed that there was delayed spindle breakage in *Dnm1*Δ cells (Figures 2a-2e).

The final time from formation to breakage of the spindle was 34.60 ± 4.03 min, while that was 42.40 ± 4.13 min in *Dnm1*Δ cells, which had extremely significant difference (p<0.01) in the two groups. The final length of spindle was 11.93 ± 0.87 μm in wild type cells, while that was 13.56 ± 1.73 μm in *Dnm1*Δ cells, which also had extremely significant difference (P<0.01) in the two groups (Figures 2e). The final time from formation to breakage of the spindle was 34.60 ± 4.03 min, while that was 42.40 ± 4.13 min in *Dnm1*Δ cells, which also had extremely significant difference (p<0.01) in the two groups. The spindle in *Dnm1*Δ cells eventually elongated with a delayed breakage by over 7 min compared to wild type cells (Figures 2d), suggesting that *Dnm1* participates in anaphase spindle elongation in addition to its established function in spindle breakage.

Cell length analysis of wild type cells and *Dnm1*Δ cells showed that the cell length of wild type cells at spindle formation point, prophase and metaphase critical point, metaphase and anaphase critical point, anaphase and telophase critical point and the end point of mitosis were 12.86 ± 1.30, 12.99 ± 1.23, 13.22 ± 1.26, 13.40 ± 1.25 and 8.46 ± 1.07 μm, respectively, while the cell length of *Dnm1*Δ cells were 14.36 ± 1.72, 14.55 ± 1.66, 14.78 ± 1.65, 14.99 ± 1.69 and 8.62 ± 0.81 μm, respectively (Figures 2g-2k). There was extremely significant difference in cell length between these two groups except the cell length at the end point of mitosis (Figures 2f).

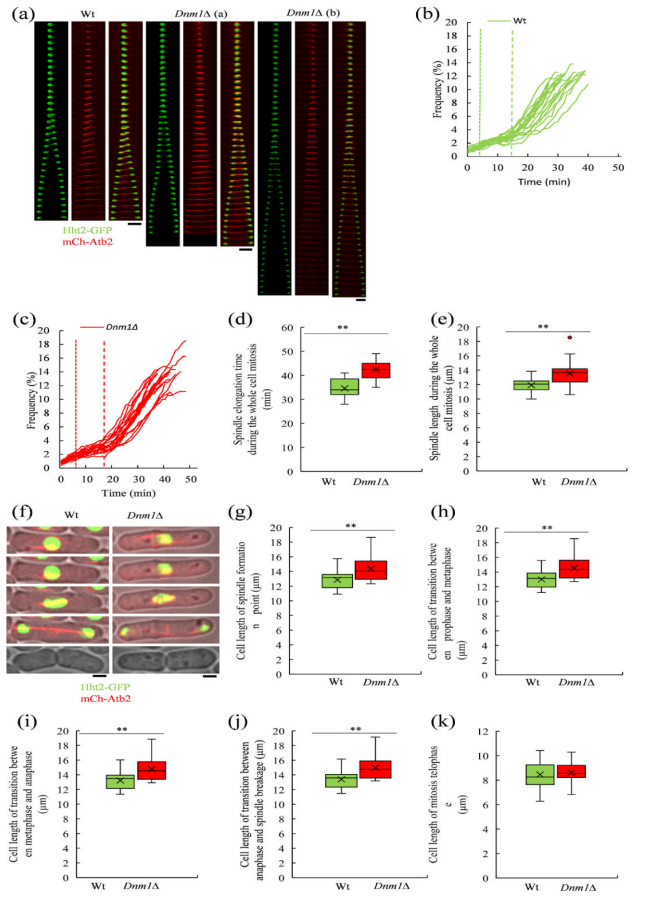

Figure 2. *The effect of Dnm1 gene deletion on spindle and cell length during cell mitosis a Spindle and chromosome dynamics of wild type and Dnm1Δ cells during the whole cell mitosis (chromosomes are marked by Hht2-GFP, spindles are marked by mCh-Atb2). a-b showed different abnormal situations in Dnm1Δ cells. Scale bar: 5 μm. b Spindle elongation analysis of wild type during cell mitosis. (n=20, n is the number of cells; The dotted line from left to right in the figure indicated the critical point between prophase and metaphase, metaphase and anaphase, respectively). c Spindle elongation analysis of Dnm1Δ cells during cell mitosis. (n=20, n is the number of cells; The dotted line from left to right in the figure indicated the critical point between prophase and metaphase, metaphase and anaphase, respectively). d Statistical analysis of the spindle elongation time of wild type and Dnm1Δ cells during the whole cell mitosis (n=20, n is the cells number). ** P<0.01. e Statistical analysis of the spindle length of wild type and Dnm1Δ cells during the whole cell mitosis (n=20, n is the cells number). ** P<0.01. f Cell morphology results of wild type and Dnm1Δ cells at spindle formation point, prophase and metaphase critical point, metaphase and anaphase critical point, anaphase and anaphase critical point and the end point of mitosis, respectively (chromosomes are marked by Hht2-GFP, spindles are marked by mCh-Atb2). Scale bar: 2 μm. The cell length analysis of wild type and Dnm1Δ cells at the spindle forming point g, prophase and metaphase critical point h, metaphase and anaphase critical point (I), anaphase and telophase critical point j and the end point of mitosis k, respectively (n=20, n is the cells number). ** P<0.01*

The effect of Dnm1 gene deletion on the spindle and chromosome in the prophase and metaphase of cell mitosis

Firstly, we analyzed spindle and chromosome dynamics in prophase and metaphase of cell division. The spindle of wild-type cells typically elongates at 0.23 ± 0.09 μm/min during prophase, with duration of prophase of 3.80 ± 1.01 min to reach a steady-state metaphase, and the spindle of wild-type cells typically elongates at 0.13 ± 0.05 μm/min during metaphase with duration of metaphase of 14.75 ± 3.43 min. In contrast, the spindle of *Dnm1*Δ cells elongates at 0.21 ± 0.08 μm/min during prophase, with duration of prophase of 4.65 ± 0.99 min to reach a steady-state metaphase, and the spindle of *Dnm1*Δ cells typically elongates at 0.12 ± 0.05 μm/min during metaphase with duration of metaphase of 15.90 ± 2.88 min (Figures 3a-3e). The duration time of prophase were significantly different between wild type and *Dnm1*Δ cells. Studies have shown that there is a significant correlation between the intensity of the fluorescent protein and gene expression level, and the fluorescent intensity can indirectly reflect the expression level of the gene at the other end of the sequence connecting it [28].

The statistical results of the fluorescence intensity of the chromosome in prophase and metaphase showed that there were no difference between wild type and *Dnm1*Δ cells, while the statistical results of the fluorescence intensity of the spindle in prophase and metaphase showed that the fluorescence intensity of the spindle in *Dnm1*Δ cells were higher than that in the wild type cells (Figurs 3f and 3g). At the same time, spindle microtubule organization and dynamics were different in *Dnm1*Δ cells compared with wild type. In the wild type, mitosis and cytoplasmic interphase microtubule disintegration occur simultaneously. In order to standardize the measurement of mitotic time, we defined the mitotic start time of 0 minute as the complete disintegration of microtubules in the cytoplasmic interphase.

In wild type, time 0 min coincides with the assembly of a microtubule “bar” (82.67 ± 6.63% of cells) or a “dot” (17.33 ± 5.77% of cells) that quickly transitions into a bar (n=20), representing the bipolar spindle. In contrast, only 43.33 ± 2.88% of *Dnm1*Δ cells exhibited bars at time 0 min. The rest exhibited delayed bipolar spindle formation, where the spindle dot occurred more frequently (21.67 ± 5.77% of cells) and took longer to form bars. Of interest, 35.00 ± 5.00% of *Dnm1*Δ cells formed transient microtubule protrusions defined as monopolar spindle (mono) (Figures 3h and 3i). No wild-type cells exhibited monopolar spindles. The results showed that spindle microtubule organization and dynamics were affected by *Dnm1* gene deletion.

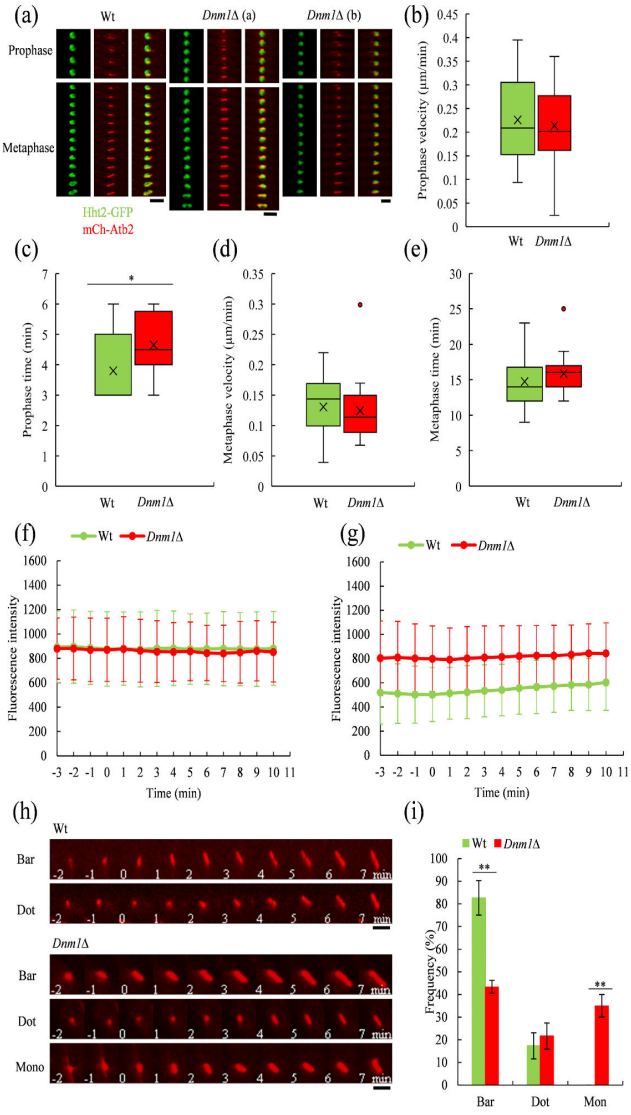

Figure 3. *The effect of Dnm1 gene deletion on the spindle and chromosome in the prophase and metaphase of cell mitosis. a Spindle and chromosome dynamics of wild type and Dnm1Δ cells at prophase and metaphase (chromosomes are marked by Hht2-GFP, spindles are marked by mCh-Atb2). a-b showed different abnormal situations in Dnm1Δ cells. Scale bar: 5 μm. b Statistical analysis of the spindle elongation rate of wild type and Dnm1Δ cells at prophase (n=20, n is the cells number). c Statistical analysis of the spindle elongation time of wild type and Dnm1Δ cells at prophase (n=20, n is the cells number). * P<0.05. d Statistical analysis of the spindle elongation rate of wild type and Dnm1Δ cells at metaphase (n=20, n is the cells number). e Statistical analysis of spindle elongation time of wild type and Dnm1Δ cells at metaphase (n=20, n is cells number). f Statistical analysis of chromosome fluorescence intensity of wild type and Dnm1Δ cells at prometaphase and metaphase (n=20, n is cell number) ("0" is the critical point of prophase and metaphase). g Statistical analysis of spindle fluorescence intensity of wild type and Dnm1Δ cells at prometaphase and metaphase (n=20, n is cell number) ("0" is the critical point of prophase and metaphase). h Morphology results of spindle formation types in wild type and Dnm1Δ cells (time "0" min is the complete disassembly of cytoplasmic interphase microtubules). Scale bar: 2 μm i Statistical analysis of spindle formation types in wild type and Dnm1Δ cells (n=20, n is cell number). ** P<0.01.*

The effect of Dnm1 gene deletion on spindles and chromosomes in the anaphase of cell mitosis

The mC-Atb2 and Hht2-GFP were also used as a detection signal for anaphase to monitor spindle elongation and chromosome segregation dynamics in cell mitosis. The spindle of wild-type cells typically elongates at 0.56 ± 0.07 μm/min during anaphase, with duration of anaphase of 16.05 ± 2.26 min. In contrast, the spindle of *Dnm1*Δ cells typically elongates at 0.50 ± 0.08 μm/min during anaphase, with duration of anaphase of 21.85 ± 3.88 min (Figures 4a-4c). Both values were also significantly different between wild type and *Dnm1*Δ cells, and duration of anaphase of wild-type were extremely significant longer than *Dnm1*Δ cells, which showed that there was delayed spindle breakage in *Dnm1*Δ cells. Chromosome segregation is an important cellular process that requires absolute fidelity because errors can lead to developmental defects and diseases. The fidelity of chromosome segregation depends to a great extent on the proper attachment of kinetochore and MT in metaphase.

Chromosome segregation requires the assembly of spindles, which are microtubules (MT)-based structures that effectively capture and separate sister chromatids during mitosis. The minus end of MT converges to the spindle pole, while the plus end of MT diverges from the opposite pole interdigitation in the middle region of spindle. There is a correlation between the mutation that changes the length of metaphase stable spindle and chromosome segregation defect. Live-cell imaging were performed on mutant strains expressing mC-Atb2 and Hht2-GFP. Two distinct chromosome behaviors were observed: normal, which the chromosome separate to opposite poles at anaphase; lagging, which the chromosome is mis-separate to one pole but are eventually corrected and separated to opposite poles (Figure 4d). We also observed that in *Dnm1*Δ wild-type cells, the spindle breaked in the form of linear-type (29.33 ± 4.66%), arch-type (41.67 ± 6.41%) and S-type (29.00 ± 5.66%), but in wild-type cells, there were only linear-type and arch-type, and the percentage of the two form were 49.67 ± 4.66% and 53.33 ± 6.44%, respectively(Figures 4e and 4f). The results showed that the loss of *Dnm1* gene could lead to abnormal spindle breakage.

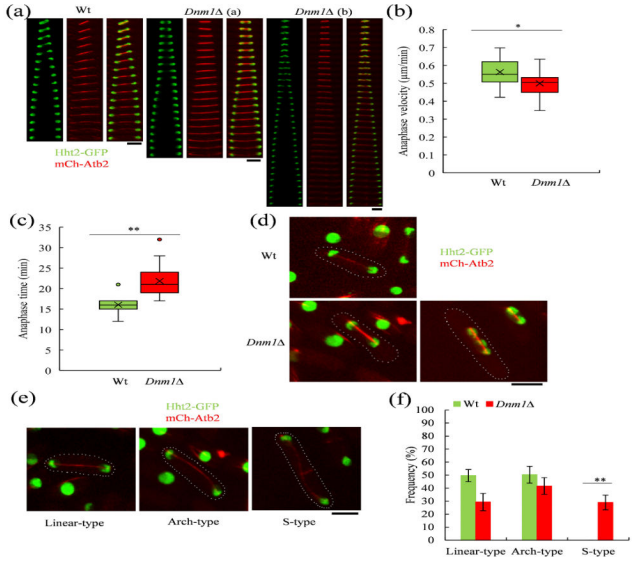

Figure 4. *The effect of Dnm1 gene deletion on spindles and chromosomes in the anaphase of cell mitosis a Spindle and chromosome dynamics of wild type and Dnm1Δ cells at anaphase (chromosomes are marked by Hht2-GFP, spindles are marked by mCh-Atb2). Scale bar: 5 μm. b Statistical analysis of the spindle elongation rate of wild type and Dnm1Δ cells at anaphase (n=20, n is the cells number). * P<0.05. c Statistical analysis of the spindle elongation time of wild type and Dnm1Δ cells at metaphase (n=20, n is the cells number). ** P<0.01. d Morphology of chromosome segregation types of wild type and Dnm1Δ cells at anaphase (chromosomes are marked by Hht2-GFP, spindles are marked by mCh-Atb2). Scale bar: 5 μm. e Morphology of spindle break types of wild type and Dnm1Δ cells at anaphase (chromosomes are marked by Hht2-GFP, spindles are marked by mCh-Atb2). Scale bar: 5 μm. f Statistical analysis of spindle break types of wild type and Dnm1Δ cells (n=20, n is the cells number). Notes: Data represented as mean ± SD. ** P<0.01.*

The effect of Dnm1 gene deletion on coenzyme in energy metabolism

Tricarboxylic acid cycle, glycolysis pathway and oxidative phosphorylation pathway are the central pathways of cell energy production. In order to further understand the energy metabolism of *Dnm1*Δ cells, the coenzyme and the energy metabolites in the process of tricarboxylic acid cycle, glycolysis pathway and oxidative phosphorylation were detected by LC-MS.

The results showed that the relative contents of flavin mononucleotide (FMN), nicotinamide adenine dinucleotide(NAD+), nicotinamide-adenine dinucleotide phosphate (NADP+), thiamine pyrophosphate (TPP) and acetyl coenzyme A (acetyl-CoA) in wild-type cells were 20.11 ± 0.31, 25.85 ± 0.08, 23.44 ± 0.37, 22.87 ± 0.18 and 19.68 ± 0.50, respectively, and those in *Dnm1*Δ cells were 19.98 ± 0.01, 25.94 ± 0.10, 15.66 ± 0.22, 23.24 ± 0.18 and 18.82 ± 0.27, respectively, which had no significant difference between these two groups (Figures 5a-5e). It was worth noting that the relative contents of nicotinamide adenine dinucleotide phosphate (NADPH) in wild-type cells was 16.37 ± 0.26, while the relative content of NADPH in *Dnm1*Δ cells was 15.66 ± 0.22 (Figure 5f), which had significant difference (P<0.05).

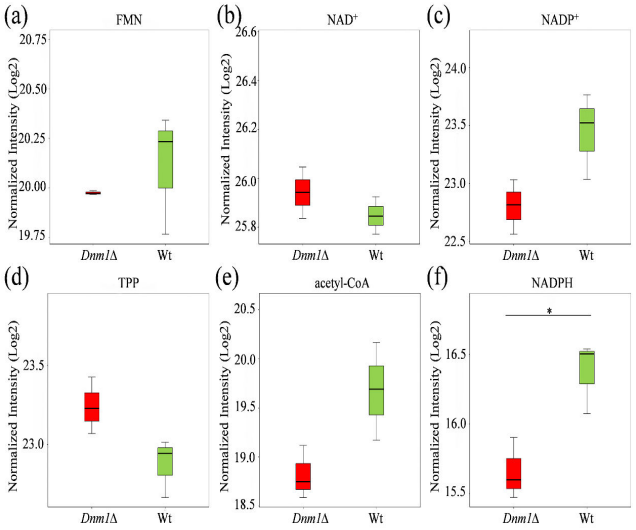

Figure 5. *The effect of Dnm1 gene deletion on coenzyme in energy metabolism a-f Statistical analysis of relative contents of FMN, NAD +, NADP+, TPP, acetyl-CoA and NADPH in wild-type and Dnm1Δ cells (n=3, the experiment was repeated three times). * P<0.05.*

The effect of Dnm1 gene deletion on intermediates of energy metabolism

Analysis of intermediates in energy metabolism indicated that some abnormalities occurred after the deletion of the *Dnm1* gene. The relative contents of D-glucose 6-phosphate, β-D-fructose 6-phosphate, citrate1, and cis-aconitate in the wild type cells were 21.9 ± 0.12, 21.19 ± 0.14, 23.40 ± 0.33 and 18.40 ± 0.15, respectively, while those in *Dnm1*Δ cells were 20.79 ± 0.06, 20.25 ± 0.21, 21.41 ± 0.17 and 16.51 ± 0.16, respectively (Figures 6a-6d), which were extremely significantly reduced in *Dnm1*Δ cells (P<0.01). The relative contents of pyruvate, isocitrate, and L-malic acid in the wild type cells were 14.07 ± 0.33, 17.17 ± 0.40 and 23.55 ± 0.47, respectively, while those in *Dnm1*Δ cells were 13.24 ± 0.33, 15.95 ± 0.21 and 22.15 ± 0.20 in *Dnm1*Δ cells, respectively, which were significantly reduced in *Dnm1*Δ cells (P<0.05) (Figures 6e-6g).

Although the relative contents of lactate, D-fructose 1,6-bisphosphate, phosphoenolpyruvate, dihydroxyacetone phosphate, oxaloacetate, α-ketoglutarate, succinate and fumarate were not significantly different in *Dnm1*Δ cells compared with wild type cells, the relative contents of those intermediates in *Dnm1*Δ cells was slightly lower than in the wild type cells (Figures 6h-6o).The above results suggested that the deletion of *Dnm1* will affect the production of intermediates in energy metabolism.

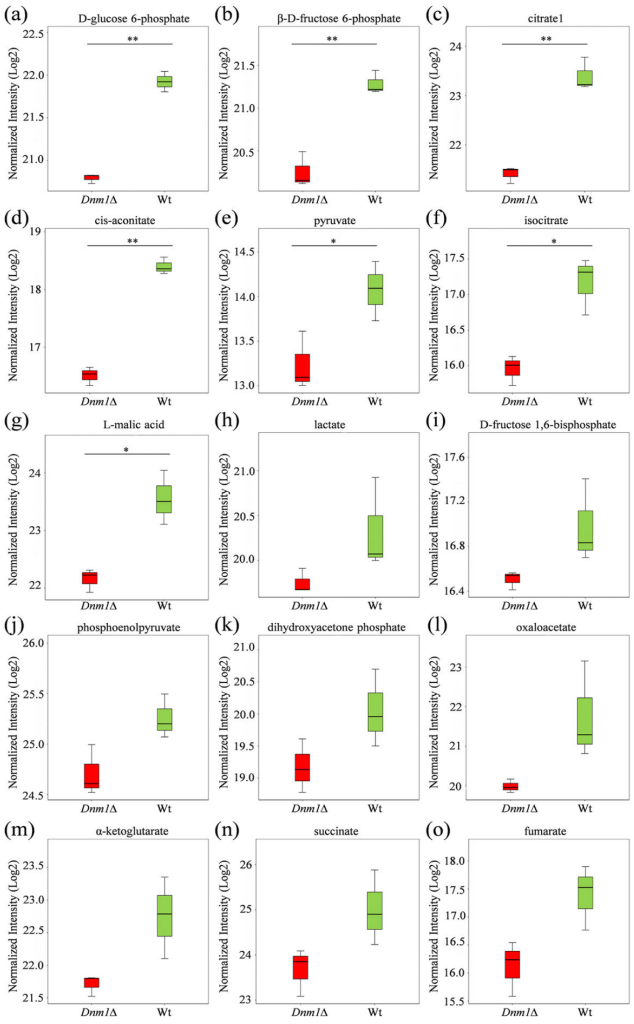

Figure 6. *The effect of Dnm1 gene deletion on intermediates of energy metabolism a-o Statistical analysis of relative contents of D-glucose 6-phosphate, β-D-fructose 6-phosphate, citrate1, cis-aconitate, pyruvate, isocitrate, L-malic acid, lactate, D-fructose 1,6-bisphosphate, phosphoenolpyruvate, dihydroxyacetone, oxaloacetate, α-ketoglutarate, succinate and fumarate in wild-type and Dnm1Δ cells (n=3, the experiment was repeated three times). * P<0.05, ** P<0.01*

The effect of Dnm1 gene deletion on energy in energy metabolism

The ultimate result of cell energy metabolism is to provides energy for cell growth and division. The results showed that the relative contents of adenosine triphosphate (ATP), adenosine diphosphate (ADP), adenosine monophosphate (AMP), guanosine triphosphate (GTP), guanosine diphosphate (GDP) and guanosine monophosphate (GMP) in the wild type cells were 21.02 ± 0.17, 24.79 ± 0.41, 26.35 ± 0.12, 16.95 ± 0.29, 20.98 ± 0.14 and 25.07 ± 0.27, respectively, while those in the *Dnm1*Δ cells were 20.21 ± 0.40, 24.85 ± 0.24, 26.39 ± 0.02, 17.06 ± 0.03, 21.41 ± 0.21 and 25.45 ± 0.06, respectively (Figures 7a-7f). It was worth noting that the relative content of ATP in the *Dnm1*Δ cells was significantly lower (P<0.05) than that of wild-type cells. The results showed that loss of *Dnm1* gene will affect ATP production.

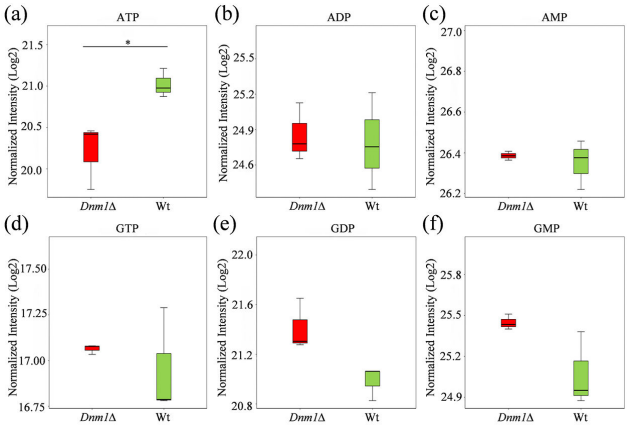

Figure 7. *The effect of Dnm1 gene deletion on energy in energy metabolism a-f Statistical analysis of relative contents of ATP, ADP, AMP, GTP, GDP and GMP in wild-type and Dnm1Δ cells (n=3, the experiment was repeated three times). * P<0.05*

Discussion

Metaphase describes a stage of mitosis in which chromosomes are attached to and oriented to bipolar spindles for later segregation. Microtubules (MTS) and their related motors play a central role in nuclear migration, and play an important role in cell division, polarity and sexual reproduction. In different cell types, the metaphase spindle maintains a characteristic constant length [23-25,29]. There are some abnormalities in *Dnm1*Δ cells. The binding of mitochondria to microtubules physically blocks the assembly of *Dnm1* around mitochondria, thus inhibiting the fission of mitochondria [30]. The interaction between microtubules and mitochondria, directly or indirectly through *Dnm1*, not only changes the arrangement of mitochondria, but also changes the behavior of microtubules. In S. cerevisiae, the inactivation of *Dnm1*p prevented the fission, and the mitochondria formed a highly interconnected tubule network. Interestingly, the mitochondrial phenotypes of fragments in *Dnm1*, mgm1 or Ugo1 mutants, and the interconnected mitochondrial phenotypes in *Dnm1*Δ cells can be alleviated when *Dnm1* is inactivated with any of them. *Dnm1*, another DRP member of fission yeast, may cause epileptic encephalopathy [31]. Spindle length statistics showed that there was delayed spindle breakage in *Dnm1*Δ cells. At the same time, spindle microtubule organization has abnormal situations in *Dnm1*Δ cells compared with wild type cells. The metaphase spindle length is thought to be regulated by the balance of pushing and pulling produced by different spindle microtubules (MTS) and their interactions with motor and MT associated proteins (MAPs (Microtubules associated proteins)). Spindle length is of great importance to the fidelity of chromosome segregation, because cells shorter or longer than normal metaphase spindles produced by deleting or inhibiting a single mitotic motor or MAPs showed chromosome segregation defects [24]. But it is not involved the deletion or inhibition of individual mitotic motors or MAPs in our research. Therefore, we have reason to believe that the loss of *Dnm1* gene from mitochondria could resulted in mitochondrial dynamics deficiency which will also contribute to the spindle

maintenance deficiency and could lead to abnormal spindle breakage in the anaphase.

Mitochondria generate ATP through oxidative phosphorylation, and also have a central role in apoptosis [32-35]. Abnormal mitochondrial division and fusion are likely to lead to energy deficiencies and ultimately to changes in cell dynamics. If fission is not controlled and balanced by fusion, the network of mitochondria becomes too fragmented which leads to glucose oxidation, mitochondrial inner membrane potential decline, leading to the downregulation of ATP production [36]. In the process of energy production in mitochondria, the abnormality of coenzyme or intermediate metabolite is likely to lead to the cell dysfunction. NADPH, mainly as a coenzyme of dehydrogenase, plays a role as a transmitter in oxidative phosphorylation and participates in a variety of anabolic reactions, such as the synthesis of lipids, fatty acids and nucleotides [37], and also regulates human cardiovascular diseases and pathophysiological processes, such as endothelial dysfunction, inflammation, hypertrophy, cell apoptosis, migration, angiogenesis and vascular and cardiac remodeling [38,39]. The NADPH production was significantly reduced compared with wild-type cells, suggesting that *Dnm1* gene deletion affected the hydrogen transfer of NADPH and the oxidative phosphorylation process. At the same time, the production of intermediates of energy metabolism showed abnormal situations in *Dnm1*Δ cells. The production of D-glucose 6-photosphate, β-D-fructose 6-photosphate, citrate1 and cis-aconitate, decreased extremely significantly ($P<0.01$), and pyruvate, isocitrate and L-malic acid decreased significantly ($P<0.05$). The production of D-glucose 6-phosphate and β-D-Fructose 6-phosphate, which appeared in the speed limiting step of glycolysis [40], are significantly reduced, suggesting that *Dnm1* gene deletion affected the key steps of glycolysis and further affects the speed of glycolysis. Pyruvate is the final product of glycolysis, and is finally imported into mitochondria as the main fuel of the tricarboxylic acid cycle. In mitochondria, pyruvate drives ATP production through a variety of biosynthetic pathways that intersect oxidative phosphorylation and the tricarboxylic acid cycle [41]. In addition, pyruvate also plays an important role in the metabolism of three major nutrients [42]. Abnormal metabolism of pyruvate plays an important role in cancer, heart failure and neurodegeneration [41]. Compared with wild type, pyruvate decreased significantly in *Dnm1*Δ cells, suggesting that *Dnm1* gene deletion can reduce the amount of pyruvate and affect ATP production and metabolism of three major nutrients. Citrate1, cis-aconitate, isocitrate and L-malic acid the important intermediates to enter the tricarboxylic acid cycle, in which citrate1 is the product of the first speed limiting step and plays a role of speed limiting. Citrate1 also plays a role of lens plasma for eyes, bones and sperm [43]. Isocitrate helps to avoid wheezing and failure of automatic resuscitation under pathological conditions [44]. L-malic acid is involved in the fourth redox in the tricarboxylic acid cycle, plays a role in promoting the capacity of the tricarboxylic acid cycle [45], plays a role in protecting myocardial ischemia / reperfusion injury, anti-inflammatory and anti-latelet aggregation [46]. Citrate1, cis-aconitate and isocitrate, L-malic acid decreased significantly suggesting that *Dnm1* gene deletion may affect the related links in the tricarboxylic acid cycle pathway and further affect energy productivity.

It was reported that mitochondrial energy production is vital for cell division in addition to other basic functions in the cell including the regulation of cell volume, solute concentration, and cellular architecture [47]. Energy levels differ at various stages of the cell cycle suggesting that there is a relationship between the abundance of energy and the cell's ability to enter a new cell cycle, which supported the hypothesis that mitochondria play an important role in cell cycle regulation [48,49]. Although the specific mechanisms between mitochondria and the cell cycle regulation is not well understood, studies have shown that low energy cell cycle checkpoints monitor the energy capability before committing to another round of cell division. There are reports showed that the abnormal mitochondrion division and fusion will make the mitochondrial network become too scattered, which lead to the deficiency of ATP production [36]. In our experiment, the results of effect of *Dnm1* gene deletion on energy in energy metabolism showed that the relative content of Adenosine 5'-triphosphate (ATP) in the *Dnm1*Δ cells were significant lower ($P<0.05$) than those in wild type cells. It is suggested that *Dnm1* gene deletion had significant effect on ATP production of cells.

Conclusion

Our experiment results indicated that the loss of *Dnm1* gene from mitochondria resulted in spindle maintenance deficiency, chromosome segregation deficiency, spindle breakage deficiency, coenzyme deficiency, intermediate metabolite deficiency and ATP production deficiency. At the moment, we are far from understanding how *Dnm1* regulates microtubule, chromosome.

Acknowledgements

This project was supported by China Scholarship Council (CSC) (201708510006 and 201708510007). The authors wish to thank Phong lab (University of Pennsylvania) for strains.

Author contributions

This study was designed and conceived by XD and YH. The experimental procedures and data analysis were carried out by XT, XD and YH. The manuscript was prepared by XT, XD and YH. All authors read and approved the final manuscript.

Conflict of interest

No competing financial interests exist.

References

1. Francy CA, Alvarez FJD, Zhou L, Ramachandran R, Mears JA. The Mechanoenzymatic Core of Dynamin-related Protein 1 Comprises the Minimal

Machinery Required for Membrane Constriction. J Biol Chem 2015; 290: 11692-11703.

2. Jourdain I, Gachet Y, Hyams JS. The dynamin related protein Dnm1 fragments mitochondria in a microtubule-dependent manner during the fission yeast cell cycle. Cell Motil Cytoskelet 2010; 66: 509-523.
3. Delerue T, Tribouillard-Tanvier D, Daloyau M, Khosrobakhsh F, Emorine LJ, Friocourt G, Belenguer P, Blondel M, Arnauné-Pelloquin L. A yeast-based screening assay identifies repurposed drugs that suppress mitochondrial fusion and mtDNA maintenance defects. Dis Model Mech 2019; 12: dmm036558.
4. Lackner LL (2014) Shaping the dynamic mitochondrial network. BMC Biol 12: 35.
5. Bertholet AM, Delerue T, Millet AM, Moulis MF, David C, Daloyau M, Arnauné-Pelloquin L, Davezac N, Mils V, Miquel MC, Rojo M, Belenguer P. Mitochondrial fusion/fission dynamics in neurodegeneration and neuronal plasticity. Neurobiol Dis 2016; 90: 3-19.
6. Chen L, Winger AJ, Knowlton AA. Mitochondrial dynamic changes in health and genetic diseases. Mol Biol Rep 2014; 41: 7053-7062.
7. Gao J, Wang L, Liu J, Xie F, Su B, Wang X. Abnormalities of Mitochondrial Dynamics in Neurodegenerative Diseases. Antioxidants 2017; 6: 25-43.
8. Burté F, Carelli V, Chinnery PF, Yu-Wai-Man P. Disturbed mitochondrial dynamics and neurodegenerative disorders. Nature Rev Neurol 2015; 11: 11-24.
9. Sajic M. Mitochondrial Dynamics in Peripheral Neuropathies. Antioxid Redox Signal 2014; 21: 601-620.
10. Zhao J, Lendahl U, Nistér M. Regulation of mitochondrial dynamics: convergences and divergences between yeast and vertebrates. Cell Mol Life Sci 2012; 70: 951-976.
11. Kim Y, Vadodaria KC, Lenkei Z, Kato T, Gage FH, Marchetto MC, Santos R. Mitochondria, Metabolism, and Redox Mechanisms in Psychiatric Disorders. Antioxid Redox Signal 2019; 31:275-317.
12. Huber N, Guimaraes S, Schrader M, Suter U, Niemann A. Charcot-Marie-Tooth disease-associated mutants of GDAP1 dissociates its roles in peroxisomal and mitochondrial fission. EMBO Rep 2013; 14: 545-552.
13. Sheffer R, Douiev L, Edvardson S, Shaag A, Tamimi K, Soiferman D, Meiner V, Saada A. Postnatal microcephaly and pain insensitivity due to a de novo heterozygous DNM1L mutation causing impaired mitochondrial fission and function. Am J Med Genet A 2016; 170: 1603-1607.
14. Rousset CI, Baburamani AA, Thornton C, Hagberg H. Mitochondria and perinatal brain injury. J Matern Fetal Neonatal Med 2012; 25: 35-38.
15. Berkovic SF, Andermann F, Shoubridge EA, Carpenter S, Robitaille Y, Andermann E, Melmed C, Karpati G. Mitochondrial dysfunction in multiple symmetrical lipomatosis. Ann Neurol 1991; 29: 566-569.
16. Naumann M, Kiefer R, Toyka KV, Sommer C, Seibel P, Reichmann H. Mitochondrial dysfunction with myoclonus epilepsy and ragged‐red fibers point mutation in nerve, muscle, and adipose tissue of a patient with multiple symmetric lipomatosis. Muscle Nerve 1997; 20: 833-839.
17. Chang CR, Manlandro CM, Arnoult D, Stadler J, Posey AE, Hill RB, Blackstone C. A lethal de novo mutation in the middle domain of the dynamin-related GTPase Drp1 impairs higher order assembly and mitochondrial division. J Biol Chem 2010; 285: 32494-32503.
18. Bleazard W, McCaffery JM, King EJ, Bale S, Mozdy A, Tieu Q. The dynamin-related GTPase Dnm1 regulates mitochondrial fission in yeast. Nat Cell Biol 1999; 1: 298-304.
19. Mears JA, Lackner LL, Fang S, Ingerman, E, Nunnari J, Hinshaw JE. Conformational changes in Dnm1 support a contractile mechanism for mitochondrial fission. Nat Struct Mol Biol 2011; 18: 20-26.
20. Karren MA, Coonrod EM, Anderson TK, Shaw JM. The role of fis1p-mdv1p interactions in mitochondrial fission complex assembly. 2005; J Cell Biol 171: 291-301.
21. Tieu Q, Okreglak V, Naylor K, Nunnari, J. The WD repeat protein, Mdv1p, functions as a molecular adaptor by interacting with dnm1p and fis1p during mitochondrial fission. J Cell Biol 2002; 158: 445-452.
22. Kuravi K, Nagotu S, Krikken AM, Sjollema K, Deckers M, Erdmann R, Veenhuis M, van der Klei IJ. Dynamin-related proteins Vps1p and Dnm1p control peroxisome abundance in saccharomyces cerevisiae. J Cell Sci 2006; 119:3994-4001.
23. Syrovatkina V, Fu C, Tran PT. Antagonistic Spindle Motors and MAPs Regulate Metaphase Spindle Length and Chromosome Segregation. Currt Biol 2013; 23: 2423-2429.
24. Dumont S, Mitchison TJ. Force and Length in the Mitotic Spindle. Curr Biol 2009; 19: R749-R761.
25. Goshima G, Scholey JM. Control of mitotic spindle length. Annu Rev Cell Dev Biol 2010; 26: 21-57.
26. Forsburg SL, Rhind N. Basic methods for fission yeast. Yeast 2006; 23: 173-183.
27. Tran PT, Paoletti A, Chang F. Imaging green fluorescent protein fusions in living fission yeast cells. Methods 2004; 33: 220-225.
28. Grignani F, Kinsella T, Mencarelli A, Valtieri M, Riganelli D, Grignani F, Lanfrancone L, Peschle C, Nolan GP, Pelicci PG. High-efficiency gene transfer and selection of human hematopoietic progenitor cells with a hybrid ebv/retroviral vector expressing the green fluorescence protein. Cancer Res 1998; 58: 14-19.
29. Mogilner A, Craig E. Towards a quantitative understanding of mitotic spindle assembly and mechanics. J Cell Sci 2010; 123: 3435-3445.
30. Mehta K, Chacko LA, Chug MK, Jhunjhunwala S, Ananthanarayanan V. Association of mitochondria with microtubules inhibits mitochondrial fission by precluding assembly of the fission protein Dnm1. J Biol Chem 2019; 294: 3385-3396.
31. von Spiczak, S., Helbig, K. L., Shinde, D. N., Huether, R., Pendziwiat, M., Lourenço, C., et al. DNM1 encephalopathy: a new disease of vesicle fission. Neurology 2017; 89: 385.
32. Jeong SY, Seol DW. The role of mitochondria in apoptosis. BMB Rep 2000; 35: 11-22.
33. Marchenko ND, Zaika A, Moll UM. Death Signal-induced Localization of p53 Protein to Mitochondria. Journal of Biol Chem 2000; 275: 16202-16212.
34. Karbowski M. Mitochondria on Guard: Role of Mitochondrial Fusion and Fission in the Regulation of Apoptosis. Adv Exp Med Biol 2010; 687: 131-142.
35. Citi V, Calderone V, Martelli A, Breschi MC, Testai L. Pathophysiological Role of Mitochondrial Potassium Channels and their Modulation by Drugs. Curre Med Chem 2018; 25: 2661-2674.
36. Bartolák-Suki E, Imsirovic J, Nishibori Y, Krishnan R, Suki B. Regulation of Mitochondrial Structure and Dynamics by the Cytoskeleton and Mechanical Factors. Int J Mol Sci 2017; 18: 1812.
37. Cave AC, Brewer AC., Narayanapanicker A, Ray R, Shah AM. NADPH oxidases in cardiovascular health and disease. Antioxid Redox Signal 2006; 8: 691-728.
38. Guzik TJ, West NEJ, Black E, McDonald D, Ratnatunga C, Pillai R, Channon KM. Vascular superoxide production by NAD(P)H oxidase: association with endothelial dysfunction and clinical risk factors. Cir Res 2000; 86: E85–E90.

39. Heymes C, Bendall JK, Ratajczak P, Cave AC, Samuel JL, Hasenfuss G, Shah AM. Increased myocardial NADPH oxidase activity in human heart failure. J Am Coll Cardiol 2003; 41: 2164-2171.
40. Jojima T, Inui M. Engineering the glycolytic pathway: a potential approach for improvement of biocatalyst performance. Bioengineered 2015; 6: 328-334.
41. Gray LR, Tompkins SC, Taylor EB. Regulation of pyruvate metabolism and human disease. Cell Mol Life Sci 2014; 71: 2577-2604.
42. Owen OE, Kalhan SC, Hanson RWThe key role of anaplerosis and cataplerosis for citric acid cycle function. J Biol Chem 2002; 277: 30409-30412.
43. Akram M. Citric Acid Cycle and Role of its Intermediates in Metabolism. Cell Biochem Biophys 2014; 68: 475-478.
44. Rivera-Angulo AJ, Peña-Ortega F. Isocitrate supplementation promotes breathing generation, gasping, and autoresuscitation in neonatal mice. J Neurosci Res 2014; 92, 375-388.
45. Srere PA. The enzymology of the formation and breakdown of citrate. Adv Enzymol Relat. Areas Mol Biol 1975; 43: 57.
46. Tang X, Liu J, Dong W, Li P, Li L, Lin C. The cardioprotective effects of citric Acid and L-malic Acid on myocardial ischemia/reperfusion injury. Evid Based Complement Alternat Med 2013; 3: 820695.
47. Sweet S, Singh G. Changes in mitochondrial mass, membrane potential, and cellular adenosine triphosphate content during the cell cycle of human leukemic (hl-60) cells. J Cell Physiol 1999; 180: 91-96.
48. Harbauer AB, Opalińska M, Gerbeth C, Herman JS, Rao S, Schönfisch B. Mitochondria. Cell cycle-dependent regulation of mitochondrial preprotein translocase. Science 2014; 346: 1109-1113.
49. Lopez-Mejia IC, Fajas L. Cell cycle regulation of mitochondrial function. Curr Opin Cell Biol 2015; 33: 19-25.

*Correspondence to

Yiling Hou

Key Laboratory of Southwest China Wildlife Resources Conservation

China West Normal University

Sichuan Province

China